

## Temperature dependent thermal conductivity of Si/SiC amorphous multilayer films

Monalisa Mazumder, Theodorian Borca-Tasciuc, Sean C. Teehan, Emilio Stinzianni, Harry Efstathiadis, and Slawa Solovyov

Citation: [Applied Physics Letters](#) **96**, 093103 (2010); doi: 10.1063/1.3337093

View online: <http://dx.doi.org/10.1063/1.3337093>

View Table of Contents: <http://scitation.aip.org/content/aip/journal/apl/96/9?ver=pdfcov>

Published by the [AIP Publishing](#)

---

### Articles you may be interested in

[Photoluminescence properties and crystallization of silicon quantum dots in hydrogenated amorphous Si-rich silicon carbide films](#)

[J. Appl. Phys.](#) **115**, 164303 (2014); 10.1063/1.4871980

[Thermal conductivity of sputtered amorphous Ge films](#)

[AIP Advances](#) **4**, 027126 (2014); 10.1063/1.4867122

[Thermal conductivity of ZnO thin film produced by reactive sputtering](#)

[J. Appl. Phys.](#) **111**, 084320 (2012); 10.1063/1.4706569

[Size-dependent electroluminescence from Si quantum dots embedded in amorphous SiC matrix](#)

[J. Appl. Phys.](#) **110**, 064322 (2011); 10.1063/1.3641989

[Structural characterization of annealed Si<sub>1-x</sub>C<sub>x</sub>/SiC multilayers targeting formation of Si nanocrystals in a SiC matrix](#)

[J. Appl. Phys.](#) **103**, 083544 (2008); 10.1063/1.2909913

---

The advertisement features a photograph of the Model PS-100 cryogenic probe station, a complex piece of scientific equipment with various mechanical components and a probe. The background is a gradient of blue. On the left, the text 'Model PS-100 Tabletop Cryogenic Probe Station' is written in white. On the right, the Lake Shore Cryotronics logo is displayed, consisting of a stylized blue and white square icon followed by the company name 'Lake Shore CRYOTRONICS' in white. Below the logo, the tagline 'An affordable solution for a wide range of research' is written in a white, italicized font.

## Temperature dependent thermal conductivity of Si/SiC amorphous multilayer films

Monalisa Mazumder,<sup>1</sup> Theodorian Borca-Tasciuc,<sup>2,a)</sup> Sean C. Teehan,<sup>3</sup> Emilio Stinzianni,<sup>3</sup> Harry Efstathiadis,<sup>3</sup> and Slowa Solovyov<sup>4</sup>

<sup>1</sup>Department of Chemical and Biological Engineering, Rensselaer Polytechnic Institute, Troy, New York 12180, USA

<sup>2</sup>Department of Mechanical, Aerospace, and Nuclear Engineering, Rensselaer Polytechnic Institute, Troy, New York 12180, USA

<sup>3</sup>College of Nanoscale Science and Engineering, University at Albany, State University of New York, Albany, New York 12203, USA

<sup>4</sup>Department of Condensed Matter Physics and Materials Science, Brookhaven National Laboratory, Upton, New York 11973, USA

(Received 16 October 2009; accepted 7 February 2010; published online 1 March 2010)

The cross-plane thermal conductivity of 22 nm period Si/SiC amorphous multilayer films deposited by magnetron sputtering and measured using a differential  $3\omega$  method was found to decrease from 2.0 W/mK at 300 K to 1.1 W/mK at 80 K. Structural disorder in each of the constituent layers of the amorphous multilayer films was confirmed by high resolution transmission electron microscopy. Estimations of the relative contributions of interface and intrinsic layer thermal resistance based on microscopic phonon transport models indicate that mean free path reductions induced by the structural disorder within the multilayer films are responsible for the observed experimental trends. © 2010 American Institute of Physics. [doi:10.1063/1.3337093]

Amorphous nanostructured multilayer films have been the focus of extensive research due to their potential applications in thermal and mechanical coating technology,<sup>1,2</sup> optoelectronics,<sup>3,4</sup> telecommunication technology<sup>5</sup> as well as in cost-effective thin-film thermoelectric power generation devices.<sup>6</sup> Amorphous multilayer films are an appealing alternative to crystalline silicon in large-area technologies due to their low-cost and low-temperature fabrication processing. Researchers have shown that amorphous multilayer films can be a potential candidate for cost-effective two-dimensional-electron-gas thermoelectric devices.<sup>6</sup> Si/SiC multilayer thin films, in particular, have been investigated for next generation optoelectronics including photodiodes and sensor arrays due to their excellent sensitivity and selectivity in vacuum ultraviolet and visible light spectrum.<sup>7-10</sup> Si/SiC multilayer films also exhibit high wear resistance and an enhanced ability to block crack propagation due to the structural differences between constituents across the multiple interfaces. These characteristics make them suitable candidates as protective coatings for optical and electronic devices.<sup>11</sup> Moreover, Si/SiC multilayer films can also serve as thermal barrier coatings for components operating in a high temperature environment like automotive components and turbine blades where maximum thermal gradient across the coating layer is desirable.<sup>1</sup> Thermal transport characterization of Si/SiC multilayer thin films is critical for efficient thermal management in the above applications. However no investigations of thermal transport in Si/SiC multilayer film systems have been reported. Here we present a temperature dependent study of the thermal conductivity of a 22 nm period Si/SiC multilayer thin film grown by physical vapor deposition and measured by a  $3\omega$  method.<sup>12-14</sup>

Deposition of Si/SiC multilayer films was carried out in a stainless steel, high vacuum reactive sputter deposition system equipped with three 7.5 cm diameter sputtering sources in a confocal configuration.<sup>15</sup> Si (99.99%) and SiC (99.95%) targets, which were independently driven by two 13.56 MHz radio frequency (rf) power supplies, were used as sputtering sources for the multilayer films and a Ta (99.99%) target, driven by a dc power supply, was used for deposition of Ta cap layers. Si/SiC multilayer films were grown on 150 mm diameter n-type Si(100) substrates in argon gas at process pressure of 4 mTorr and substrate temperature of 27 °C using power density of 4.38 W/cm<sup>2</sup> and 5.48 W/cm<sup>2</sup> for Si and SiC, respectively. A set of two samples of 30 and 50 periods, each with a 30 nm thick *in situ*-deposited Ta cap layer on the top of the multilayer film, were grown for thermal conductivity measurements. A mirror sample consisting of 30 periods of Si/SiC and without any Ta cap layer was also deposited for TEM investigations. The growth rate of the Si layer was 6 nm/min while that of SiC layer was about 1.3 nm/min. The resulting multilayer films were characterized in terms of thickness and interface roughness and density by X-ray reflection (XRR) using a Rigaku Ultima III X-ray diffractometer. The thickness of the Si and SiC individual layers in the multilayer configuration was found to be 14.3 nm and 8 nm, respectively. The film thickness non-uniformity across the 150 mm Si wafer was measured to be 3.8%. Cross-sectional transmission electron microscopy (TEM) analysis, using JOEL 2010-F FEG TEM operated at 200 kV, shows periodic stacking of the constituent layers of the multilayer film as shown in Fig. 1(a). The high resolution TEM (HRTEM) micrograph in Fig. 1(b) as well as the diffraction pattern in the inset of Fig. 1(a) reveals the amorphous nature of the layers. Only a few nanometers of epitaxial growth in the first Si layer, adjacent to the substrate, can be observed in Fig. 1(b).

<sup>a)</sup>Author to whom correspondence should be addressed. Electronic mail: borcat@rpi.edu.

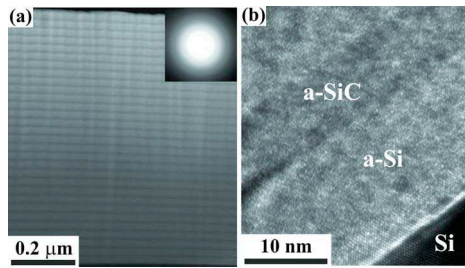


FIG. 1. (Color online) (a) Low resolution TEM Micrograph of the Si/SiC multilayer film with 30 periods each consisting of alternating layers of 14 nm Si and 8 nm SiC. The inset is the diffraction pattern of a selected area in the middle of the stack indicating the structure is amorphous. (b) HRTEM micrograph confirming the amorphous nature of the film. A few nanometers of epitaxial growth are observed only in the first Si layer adjacent to the substrate.

A differential  $3\omega$  method<sup>16</sup> was employed to perform the thermal conductivity measurements on the Si/SiC multilayer films. In our case the smaller thickness (30 periods) multilayer film sample serves as the reference while the larger thickness (50 periods) multilayer film sample is used to extract the effective thermal conductivity across 20 periods of the Si/SiC multilayer film. The sample configuration is shown in the inset of Fig. 2(a). An insulation layer of  $\sim 100$  nm silicon nitride ( $\text{SiN}_x$ ) was deposited by plasma enhanced chemical-vapor deposition (PECVD) at  $300^\circ\text{C}$ .

The temperature-dependent thermal conductivity measurements were carried out in a cryostat in the temperature range from 80 K to room temperature. During the  $3\omega$  mea-

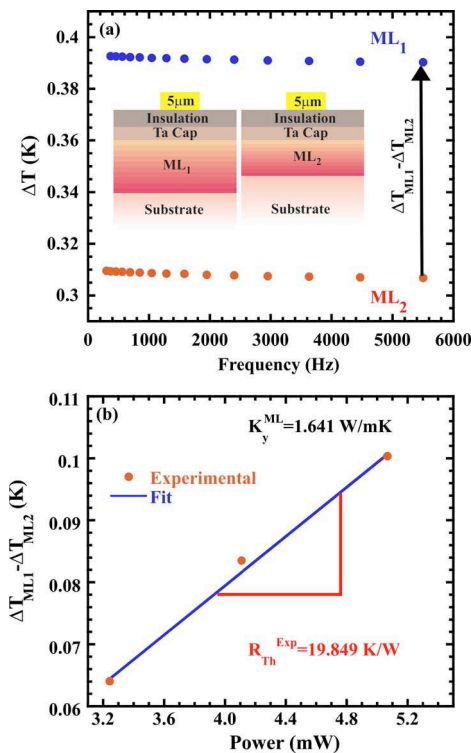


FIG. 2. (Color online) (a) ac temperature amplitude as a function of heating current frequency measured at 150 K for multilayer film samples with 50 periods ( $\text{ML}_1^S$ ) and 30 periods ( $\text{ML}_2^R$ ), respectively. The inset illustrates a schematic representation of the measured multilayer film samples. (b) The measured temperature difference between the samples is linear with dissipated power. The slope of the fitted line gives the experimental thermal resistance across 20 periods of the multilayer film and is used to determine the multilayer film thermal conductivity.

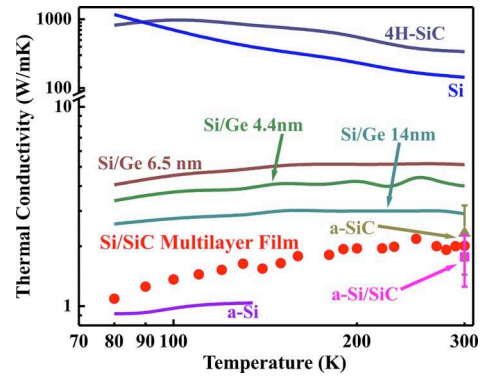


FIG. 3. (Color online) Thermal Conductivity of Si/SiC multilayer film compared to that of crystalline and amorphous Si and SiC, as well as to thermal conductivity of Si/Ge superlattices from literature. At room temperature the thermal conductivity of the multilayer film is within the range estimated from classical heat conduction modeling across an a-Si/a-SiC layer of similar composition as the Si/SiC multilayer film. The values of thermal conductivity of amorphous Si, single crystal and amorphous SiC, and single crystal Si/Ge superlattices are from Refs. 12 and 18–22.

surements, the temperature variations in the cryogenic chamber were within 0.1 K of setpoint.

Figure 2(a) shows the ac temperature amplitude in the multilayer film samples as a function of input frequency for an identical input power and  $5\ \mu\text{m}$  wire width. The measured temperature difference between the thinner multilayer film, referred to as reference sample, and the thicker multilayer film sample was used to determine the intrinsic thermal conductivity of the multilayer film as described below. The differential temperature is relatively constant between 2500 and 5500 Hz. Its averaged value over the experimental frequency range is linear with input power as shown in Fig. 2(b). The slope of the fitted line in Fig. 2(a) gives an experimental estimate of the thermal resistance across 20 periods of the multilayer film. The slope thermal resistance method has the advantage of compensating for offsets in the experimental data. Fitting this thermal resistance with a 2D heat conduction model<sup>16</sup> yields the effective thermal conductivity of the multilayer film. The measured effective thermal conductivity of the multilayer film is minimally influenced by contributions from insulation and cap layer's thermal conductivity. The validity of this assumption was assessed by an analysis of the sensitivity of the differentially measured thermal resistance of the multilayer film toward variations in the thermophysical properties of the adjacent layers. It was found that an order of magnitude variation in the thermal conductivity of the Si substrate, introduced only 0.3% change in the determined multilayer film thermal conductivity. Likewise, a 60% change in the input thermal conductivity of the insulation layer incurs only a 6% change. Hence, in this work, the reported literature value of thermal conductivity of silicon nitride was used.<sup>17</sup> Even less sensitivity, ( $<0.05\%$ ), was observed due to the uncertainty in thermal conductivity of the tantalum cap layer which was neglected in subsequent data analysis. Therefore the differential  $3\omega$  approach significantly reduces the uncertainty arising from the thermophysical properties of the constituent layers.

Figure 3 shows the temperature dependent effective cross-plane thermal conductivity of the Si/SiC multilayer film compared with literature values of thermal conductivities for single crystal and amorphous Si<sup>12</sup> and SiC<sup>18–20</sup> and epitaxial Si/Ge superlattices.<sup>21,22</sup> The thermal conductivity

of the Si/SiC multilayer film varies from  $\sim 2.0$  W/mK at 300 K to 1.1 W/mK at 80 K with a relatively small variation of 19% in the temperature range from 300 to 130 K and a stronger variation of 33% between 130 and 80 K. The experimental uncertainty of the thermal conductivity is conservatively estimated to be  $<10\%$ , with film thickness non-uniformity and insulation layer thermal conductivity being the main contributors to uncertainty. Compared to Si/Ge superlattice system, the Si/SiC multilayer film has significantly lower thermal conductivity values but shows a similar increasing trend with temperature. In crystalline superlattice systems this behavior is due to limitations of the mean free path (MFP) of phonons by scattering at the superlattice interfaces in conjunction with the increase in heat capacity. In contrast, TEM indicates that our Si/SiC multilayer film has an amorphous structure in which case the MFP reduction could be caused mainly by disorder in each layer rather than interface scattering. The MFP in the measured Si/SiC multilayer film layers as well as the contribution to thermal transport due to the interface thermal resistance (ITR) at the Si/SiC interfaces were estimated in order to assess the validity of this assumption. The effect of ITR was evaluated based on the analytical model described by Prasher *et al.*<sup>23</sup> The thermal boundary resistance was estimated to be  $4.77 \times 10^{-7}$  m<sup>2</sup> K/W for one interface leading to a total ITR of  $9.55 \times 10^{-5}$  m<sup>2</sup> K/W which is only 4.84% of the experimentally measured total thermal resistance ( $R^{\text{Th}}$ ). Furthermore, the phonon MFP in each layer of the multilayer film is estimated based on kinetic theory considering the phonon group velocity and the contribution of acoustic phonon modes to the volumetric heat capacity, obtained from approximate phonon dispersion relations,<sup>24</sup> rather than using sound velocity and total specific heat, respectively. This approach gives a phonon MFP of 260.4 nm<sup>24</sup> at room temperature and 4.2  $\mu\text{m}$  at 80 K in bulk single crystal Si, but in amorphous silicon its values range from only 1.9 nm at 300 K to 3.4 nm at 80 K, much smaller than the thickness of 14 nm of the Si layers in the Si/SiC multilayer film. It is to be noted, however, that the above MFP estimates for amorphous Si at 300 and 80 K are, respectively, 6.3 and 3.6 times higher than predictions based on the Debye model.<sup>24</sup> For amorphous SiC the thermal conductivity at room temperature is reported in the range of 1.44 to 3.5 W/mK.<sup>19,20</sup> The Debye model predicts a MFP between 0.168 to 0.408 nm in amorphous SiC at room temperature. Assuming a similar discrepancy between the Debye and dispersion models as seen in the case of Si, the phonon MFP in amorphous SiC is between 1.06 to 2.58 nm, considerably smaller than the 8 nm thickness of the SiC layer in the multilayer film. Employing classical heat conduction modeling, the thermal conductivity of a composite made of amorphous Si and SiC with similar composition as the measured multilayer film is in the range of 1.25 to 2.28 W/mK, comparable to the experimental value of 2.01 W/mK for the multilayer film shown in Fig. 3. This good match indicates that in the measured Si/SiC system size effects do not play a major factor to thermal transport at room temperature due to the amorphous nature of the layers in the multilayer structure.

In summary, this work reports the cross-plane thermal conductivity of Si/SiC multilayer films. The thermal conductivity varies from 2.01 W/mK at 300 K to 1.09 W/mK at 80 K. The interface thermal resistance between the Si and SiC layers of the multilayer film contributes only 5% to the experimentally measured total thermal resistance. Phonon MFP estimates indicate that at room temperature size effects do not play a major factor to thermal transport in the amorphous multilayer structures. An estimate of multilayer film thermal conductivity based on classical heat conduction modeling across amorphous multilayer films agrees well with the measured thermal conductivity at room temperature. The amorphous structure in each layer of the multilayer films was confirmed by TEM investigations.

The authors (M.M. and T.B.T.) acknowledge financial support by the National Science Foundation Grant No. CBET-0348613. Research was carried out in part at the Center for Functional Nanomaterials, Brookhaven National Laboratory, which is supported by the U.S. Department of Energy, Office of Basic Energy Sciences, under Contract No. DE-AC02-98CH10886.

- <sup>1</sup>N. P. Padture, M. Gell, and E. H. Jordan, *Science* **296**, 280 (2002).
- <sup>2</sup>E. Bertran, G. Viera, E. Martinez, J. Esteve, Y. Maniette, J. Farjas, and P. Roura, *Thin Solid Films* **377–378**, 495 (2000).
- <sup>3</sup>H. Steibig, R. A. Street, D. Knipp, M. Krause, and J. Ho, *Appl. Phys. Lett.* **88**, 013509 (2006).
- <sup>4</sup>D. Caputo, G. de Cesare, A. Nascetti, and M. Tucci, *IEEE Trans. Electron Devices* **55**, 452 (2008).
- <sup>5</sup>M. Vieira, P. Louro, M. Fernandes, M. A. Vieira, A. Fantoni, and M. Barata, *Thin Solid Films* **517**, 6435 (2009).
- <sup>6</sup>H. Ohta, R. Huang, and Y. Ikuhara, *Phys. Status Solidi (RRL)* **2**, 105 (2008).
- <sup>7</sup>G. de Cesare, F. Irrera, F. Lemmi, and F. Palma, *Appl. Phys. Lett.* **66**, 1178 (1995).
- <sup>8</sup>G. de Cesare, F. Irrera, F. Palma, M. Tucci, E. Jannitti, G. Naletto, and P. Nicolosi, *Appl. Phys. Lett.* **67**, 335 (1995).
- <sup>9</sup>P. Mandracci, F. Giorgis, C. F. Pirri, and M. L. Rastello, *Rev. Sci. Instrum.* **70**, 2235 (1999).
- <sup>10</sup>M. Topič, H. Stiebig, M. Krause, and H. Wagner, *Appl. Phys. Lett.* **78**, 2387 (2001).
- <sup>11</sup>E. Bertran, E. Martinez, G. Viera, J. Farjas, and P. Roura, *Diamond Relat. Mater.* **10**, 1115 (2001).
- <sup>12</sup>D. G. Cahill, H. E. Fischer, T. Klitsner, E. T. Swartz, and R. O. Pohl, *J. Vac. Sci. Technol. A* **7**, 1259 (1989).
- <sup>13</sup>D. G. Cahill, *Rev. Sci. Instrum.* **61**, 802 (1990).
- <sup>14</sup>D. G. Cahill, M. Katiyar, and J. R. Abelson, *Phys. Rev. B* **50**, 6077 (1994).
- <sup>15</sup>T. Yu, H. Efstathiadis, R. Matyi, and P. Haldar, *Mater. Res. Soc. Symp. Proc.* **886**, 4 (2004).
- <sup>16</sup>T. Borca-Tasciuc, A. R. Kumar, and G. Chen, *Rev. Sci. Instrum.* **72**, 2139 (2001).
- <sup>17</sup>S.-M. Lee and D. G. Cahill, *J. Appl. Phys.* **81**, 2590 (1997).
- <sup>18</sup>D. T. Morelli, J. P. Heremans, C. P. Beetz, W. S. Yoo, and H. Matsunami, *Appl. Phys. Lett.* **63**, 3143 (1993).
- <sup>19</sup>S. R. Choi, D. Kim, S.-H. Choa, S.-H. Lee, and J.-K. Kim, *Int. J. Thermophys* **27**, 896 (2006).
- <sup>20</sup>L. L. Snead and S. J. Zinkle, *Nucl. Instrum. Methods Phys. Res. B* **191**, 497 (2002).
- <sup>21</sup>T. Borca-Tasciuc, W. Liu, J. Liu, T. Zeng, D. W. Song, C. D. Moore, G. Chen, K. L. Wang, and M. S. Goorsky, *Superlattices Microstruct.* **28**, 199 (2000).
- <sup>22</sup>S.-M. Lee, D. G. Cahill, and R. Venkatasubramanian, *Appl. Phys. Lett.* **70**, 2957 (1997).
- <sup>23</sup>R. S. Prasher and P. E. Phelan, *J. Appl. Phys.* **100**, 063538 (2006).
- <sup>24</sup>G. Chen, *Phys. Rev. B* **57**, 14958 (1998).